New insights on pharmacological activity of imidazo-pyrazole scaffold

Andrea Spallarossa,[a] Federica Rapetti,[a] Maria Grazia Signorello,[b] Camillo Rosano,[c] Erika Iervasi,[c] Marco Ponassi,[c] Chiara Brullo*[a]

[a] Prof. A. Spallarossa, Dr. F. Rapetti, Prof. C. Brullo
Department of Pharmacy, Section of Medicinal Chemistry
University of Genoa
Viale Benedetto XV 3
I-16132 Genova, Italy
E-mail: chiara.brullo@unige.it

[b] Prof. M.G. Signorello
Department of Pharmacy, Biochemistry Laboratory
University of Genoa
Viale Benedetto XV 3
I-16132 Genova, Italy

[c] Dr. C. Rosano, Dr. E. Iervasi, Dr. M. Ponassi
IRCCS Ospedale Policlinico San Martino Unit
Proteomics and Mass Spectrometry
L.go. R. Benzi, 10
I-16132 Genova, Italy

Supporting information for this article is given via a link at the end of the document.

Abstract: In previous studies, we synthesized different imidazo-pyrazoles **1** and **2** with interesting anti-cancer, anti-angiogenic and anti-inflammatory activities. To further extend the structure-activity relationships of imidazo-pyrazole scaffold and to identify novel anti-proliferative/anti-inflammatory agents potentially active with multi-target mechanisms, a library of compounds **3-5** has been designed and synthesized. The chemical modifications characterizing the novel derivatives include: i) decoration of the catechol ring with groups with different electronic, steric and lipophilic properties (compounds **3**); ii) insertion of a methyl group on C-6 of imidazo-pyrazole scaffold (compounds **4**); iii) shift of the acylhydrazonic substituent from position 7 to 6 of the imidazo-pyrazole substructure (compounds **5**). All synthesized compounds were tested against a panel of cancer and normal cell lines. Derivatives **3a**, **3e**, **4c**, **5g** and **5h** showed IC_{50} values in the low micromolar range against selected tumor cell lines and proved to have antioxidant properties, being able to inhibit ROS production in human platelet. In silico calculation predicted favourable drug-like and pharmacokinetic properties for the most promising compounds. Furthermore, molecular docking and molecular dynamic simulations suggested the ability of most active derivative **3e** to interact with colchicine binding site in the polymeric tubulin α/tubulin β/stathmin4 complex.

Introduction

Cancer is a multifactorial disease characterized by unchecked cell proliferation that quickly infiltrate in tissues and organs. Although many innovative therapies have been introduced to date, the onset of drug resistance is expected to cause a large increase in cancer mortality in the next few years.[1]

Although inflammation and cancer are often associated, the involvement of phlogosis and immunosurveillance in cancer development and progression has been established only in recent decades.[2,3] Indeed, it has been evaluated that about 20% of cancers are related to inflammation and furthermore solid neoplasms are preceded by tissue inflammation.[4-6] Moreover, different studies demonstrated that neutrophil migration (chemotaxis) and subsequent production of cytokines, most involved in inflammation process, play also a central role in cancer progression and onset;[2,5]. Collectively all these data support a close relationship between inflammation and cancer.

Differently from other heterocyclic compounds,[7,8] imidazo-pyrazole scaffold represents a chemotype not deeply investigated in medicinal chemistry and could provide important hits for the identification of novel pharmacologically active compounds.

In our previous ~~works~~studies, we identified a large library of imidazo-pyrazoles differently decorated on N1, C-6 and C-7 position (compounds **1**, Figure 1) able to contrast inflammation by blocking neutrophils chemotaxis and inhibiting ERK1/2, AKT and p38MAPK phosphorylation.[9,10] Moreover, some derivatives proved to reduced angiogenesis process in VEGF-stimulated human umbilical vein endothelial cells (HUVEC) and in neuroblastoma cell lines.[11,12] More recently, other imidazo-pyrazoles (compounds **2**, Figure 1), sharing with a number of new anti-cancer drugs a differently decorated acylhydrazone moiety,[13-15] evidenced interesting anti-proliferative and antioxidant properties.[16,17] Interestingly, compounds with bulky substituents at para position of catechol ring (derivatives **2a** and **2b**, Figure 2) evidenced a remarkable anti-cancer activity through the interaction with different intracellular systems, including tubulin,[16] whereas derivatives characterized by a smaller substituent (e.g., **2c**, Figure 2) inhibited reactive oxygen species (ROS) production.[17]

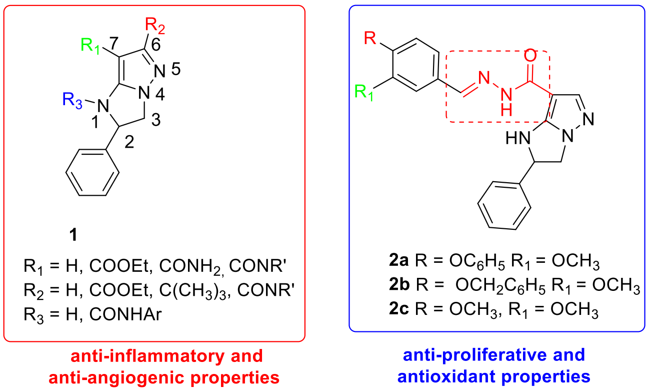
R2
6
R1
7
5
N
N
4
R3
N
1
3
2
1
R_1 = H, COOEt, $CONH_2$, CONR'
R_2 = H, COOEt, $C(CH_3)_3$, CONR'
R_3 = H, CONHAr
anti-inflammatory and
anti-angiogenic properties
R
R1
N
N
H
O
HN
N
N
2a R = OC_6H_5 R_1 = OCH_3
2b R = $OCH_2C_6H_5$ R_1 = OCH_3
2c R = OCH_3, R_1 = OCH_3
anti-proliferative and
antioxidant properties

Figure 1. Structure of previous synthesized imidazo-pyrazoles **1** and **2** and related biological properties.

To further extend the structure-activity relationships (SARs) of derivatives **2** and to identify novel imidazo-pyrazoles endowed with anti-proliferative/anti-inflammatory properties, we designed and synthesized a new library (twenty compounds) of imidazo-pyrazole compounds **3-5** (Figure 2, Table 1). In the new derivatives we introduced the following chemical modifications: (i) decoration of the catechol ring with groups with different electronic, steric and lipophilic properties (compounds **3**); (ii) insertion of a methyl group on C-6 of imidazo-pyrazole scaffold (compounds **4**); (iii) shift of the acylhydrazonic substituent from position 7 to position 6 of the imidazo-pyrazole substructure (compounds **5**).

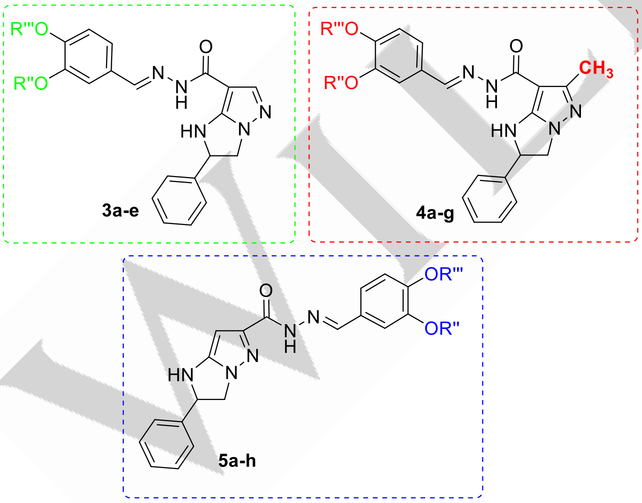
R'''O
R''O
N
N
H
O
HN
N
N
3a-e
R'''O
R''O
N
N
H
O
CH3
HN
N
N
4a-g
O
N
N
H
OR'''
OR''
HN
N
N
5a-h

Figure 2. Structure of new synthesized compounds **3-5**.

To confirm the biological activity of imidazo-pyrazole core, already observed in the previous compounds **1** and **2**, we firstly submitted newly synthesized derivatives **3-5** to a preliminary screening to evaluate their anti-proliferative action. Then, for the most promising molecules, we assessed cytotoxicity, ROS production inhibition and in silico pharmacokinetics and drug-likeness properties. Finally, as previous imidazo-pyrazoles **2a,b** resulted active as tubulin polymerization inhibitors,[16] molecular docking and molecular dynamic simulations on tubulin system were carried out for the most potent anti-proliferative compounds.

Results and Discussion

Chemistry

The desired compounds **3-5** were synthesized through the four-step sequential procedure reported in Scheme 1.

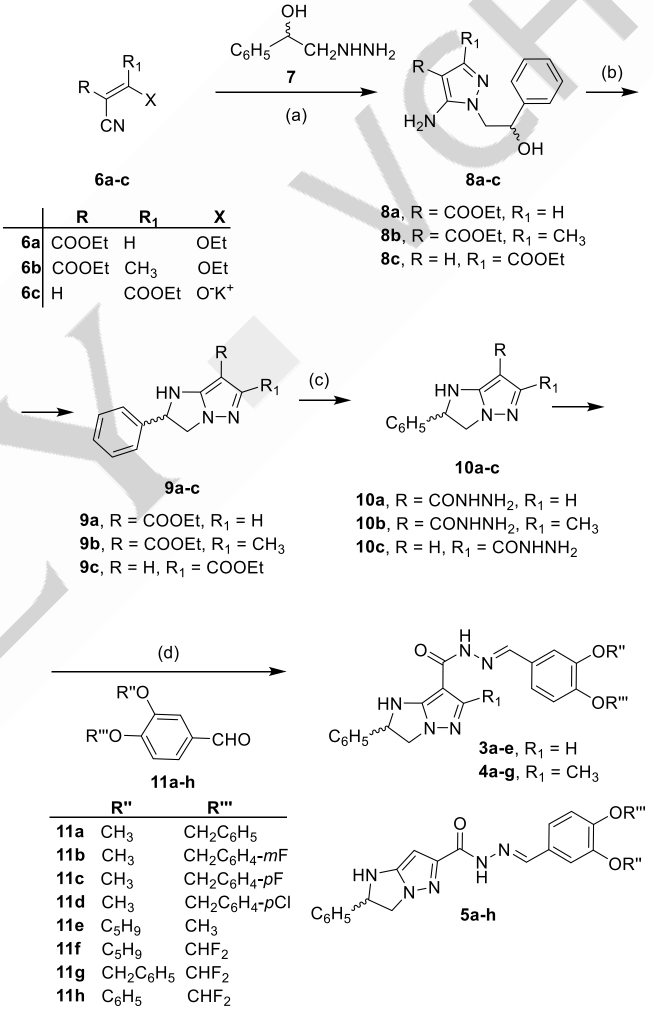
OH
C_6H_5
CH_2NHNH_2
7
(a)
R
R1
X
CN
6a-c
R
R1
N
N
H2N
OH
8a-c
(b)
R
R1
HN
N
N
9a-c
(c)
R
R1
HN
C6H5
N
N
10a-c
(d)
R''O
R'''O
CHO
11a-h
O
N
N
H
OR''
OR'''
R1
HN
C6H5
N
N
3a-e, R_1 = H
4a-g, R_1 = CH_3
O
N
N
H
OR'''
OR''
HN
C6H5
N
N
5a-h

	R	R_1	X
6a	COOEt	H	OEt
6b	COOEt	CH_3	OEt
6c	H	COOEt	O^-K^+

8a, R = COOEt, R_1 = H
8b, R = COOEt, R_1 = CH_3
8c, R = H, R_1 = COOEt

9a, R = COOEt, R_1 = H
9b, R = COOEt, R_1 = CH_3
9c, R = H, R_1 = COOEt

10a, R = $CONHNH_2$, R_1 = H
10b, R = $CONHNH_2$, R_1 = CH_3
10c, R = H, R_1 = $CONHNH_2$

	R''	R'''
11a	CH_3	$CH_2C_6H_5$
11b	CH_3	$CH_2C_6H_4$-*mF*
11c	CH_3	$CH_2C_6H_4$-*pF*
11d	CH_3	$CH_2C_6H_4$-*pCl*
11e	C_5H_9	CH_3
11f	C_5H_9	CHF_2
11g	$CH_2C_6H_5$	CHF_2
11h	C_6H_5	CHF_2

Scheme 1. Synthesis of compounds **3-5**. Reagents and conditions: (a) Toluene, 70-80 °C, 8h (**8a**, **8c**) or absolute ethanol (abs. EtOH), reflux (**8b**); (b) conc. H_2SO_4, 0 °C, 10 min., then concentrated ammonium solution (conc. NH_4OH), r.t.; (c) $NH_2NH_2 \cdot H_2O$, 120-130 °C, 3-4h; (d) abs. EtOH, **11a-h**, reflux 1-18h.

In particular, the condensation of the proper ethyl cyanoacrylate **6a-c** with 2-phenyl-1-hydrazinoethanol **7**[18] led to the isolation of 3-amino pyrazoles **8a-c**, as previously reported.[8,19] The dehydration of pyrazoles **8a-c** with concentrated sulphuric acid (H_2SO_4) allowed the isolation of imidazo-pyrazole racemic esters **9a-c**, [7,8] that were then transformed in the corresponding hydrazides **10a-c** by the reaction with hydrazine hydrate

($NH_2NH_2 \cdot H_2O$). Finally, the condensation between carbohydrazide intermediates **10** and the suitable benzaldehydes **11a-h** (properly prepared according to literature methods)[17, 20-23] led to the formation of the desired compounds **3-5** in good-to-moderate yields (Table 1).

Interestingly, the adopted reaction conditions for the formation of the acylhydrazone functionality proved to be stereoselective. In fact, although the condensation between compounds **10** and **11** could potentially lead to the formation of *E*/*Z* mixtures, only derivatives *E* were isolated, as assessed by NMR spectral analyses. As recently reported for similar hydrazones [16,17], *E*-geometry was definitively assigned based on the chemical shift of the acylhydrazone proton atom. In particular, a chemical shift for CONH proton lower than 12 ppm (as in our case) was assigned to the *E* configuration, whereas δ values higher than 15.5 ppm indicated a *Z* isomer.[24]

Table 1. Decorations on the new synthesized compounds **3-5**.

Compd.	R''	R'''	Yield (%)
3a	C_6H_5	CHF_2	49
3b	$CH_2C_6H_5$	CHF_2	50
3c	CH_3	$CH_2C_6H_4$-*p*F	62
3d	CH_3	$CH_2C_6H_4$-*m*F	47
3e	CH_3	$CH_2C_6H_4$-*p*Cl	52
4a	C_5H_9	CH_3	68
4b	C_5H_9	CHF_2	68
4c	C_6H_5	CHF_2	50
4d	$CH_2C_6H_5$	CHF_2	87
4e	CH_3	$CH_2C_6H_4$-*p*F	92
4f	CH_3	$CH_2C_6H_4$-*m*F	50
4g	CH_3	$CH_2C_6H_4$-*p*Cl	58
5a	C_5H_9	CH_3	88
5b	C_5H_9	CHF_2	42
5c	C_6H_5	CHF_2	42
5d	$CH_2C_6H_5$	CHF_2	79
5e	CH_3	$CH_2C_6H_5$	40
5f	CH_3	$CH_2C_6H_4$-*p*F	62
5g	CH_3	$CH_2C_6H_4$-*m*F	84
5h	CH_3	$CH_2C_6H_4$-*p*Cl	92

Anti-proliferative activity

To confirm the anti-cancer activity of imidazo-pyrazole core, imidazo-pyrazoles **3-5** were tested at a fixed concentration of 10 μM against eight different cancer cell lines (namely, MCF7 breast adenocarcinoma, SKOV-3 ovarian adenocarcinoma, Hep-G2 hepatocellular carcinoma, SK-Mel28 cutaneous melanoma, MDA-MB-231 breast adenocarcinoma, SK-BR3 breast adenocarcinoma, HeLa cervix epithelioid carcinoma and A549 lung carcinoma) using Cisplatin (Cis-Pt) as reference compound. As reported in Table 2, selected compounds showed significative anti-proliferative activity (cancer cell growth percentage < 50% at 10 μM concentration), resulting equally active or more effective than the reference compound. In detail, compounds **3**, more strictly related to lead structures **2a,b** (Figure 1), showed very interesting anti-proliferative activity and derivatives **3c**, **3d** and **3e**, sharing an halogen-substituted benzyloxy ring, potently inhibited the proliferation of A549, HeLa, SK-Mel28, MCF7 and SKOV-3 cell lines.

Derivatives **4**, bearing an additional methyl group at C-6 position of the imidazo-pyrazole scaffold, resulted less active than compounds **3** against the considered panel of cell lines. However, compounds **4b** and **4d** selectively blocked cervix epithelioid carcinoma (HeLa cell line), whereas **4c** shows inhibitory activity on HeLa, Hep-G2 and SK-Mel28 proliferation. Conversely, **4e** broadly affect the proliferation of the considered cell lines.

Finally, among compounds **5**, bearing the acylhydrazone linker at position 6, ~~derivatives~~ **5f**, **5g** and **5h** showed interesting results (Table 2). In detail, **5f** was effective and selective towards hepatocellular carcinoma (Hep-G2 cell line), whereas **5g** exhibited strong action particularly against breast cancer cells MCF7 and MDA-MB2311. Compound **5h**, a close analogue of **2a** with an additional chlorine atom on benzyloxy substituent, strongly inhibited the proliferation of lung carcinoma (A549) and breast cancer (MBA-MB321) cells.

Collectively, the most potent imidazo-pyrazoles shared a difluoromethoxy substituents at para position of catechol moiety and a phenoxy group in meta position (derivatives **3a** and **4c**) or a 3-methoxy-4-substituted benzyloxy substructure (compounds **3e**, **4e**, **5g** and **5h**). In particular, the 4-chloro-benzyloxy substituted compounds **3e** and **5g** showed a broad spectrum of anti-proliferative activity, whereas the presence of a smaller substituents (phenoxy and difuoromethoxy), as in compounds **3a** and **4c,** resulted in a more specific and selective anti-cancer action.

To further characterize the anti-proliferative profile of the most active derivatives, the IC$_{50}$ values of compounds **3a**, **3e**, **4c**, **5g** and **5h** were determined on selected cancer cell lines (Table 3).

The tested compounds showed widespread and significant anti-cancer activity, thus confirming imidazo-pyrazole scaffold as a valuable ~~moiety~~ chemo-type for the development of novel anti-proliferative agents. In particular, **3a** showed a IC$_{50}$ value in the low micromolar range against SK-Mel 28, HeLa and A549 cancer cell lines (5.49 μM, 6.30 μM and 6.71 μM, respectively), while **3e** was highly active against the ovarian adenocarcinoma (SKOV-3) and lung carcinoma (A549) cell lines (IC$_{50}$ values lower than 3 μM). As anticipated by growth percentage values (Table 2), derivative **5h** showed a widespread activity (IC$_{50}$ values < 10 μM) against all considered cell lines, being highly effective against lung carcinoma A549 (IC$_{50}$ = 2.57 μM), cutaneous melanoma SK-Mel 28 (IC$_{50}$ = 4.94 μM) and breast cancer MDA-MB231 (IC$_{50}$ = 5.02 μM) lines. Noteworthy **3e** and **5h** are both characterized by a methoxy group in position 3 and the 4-chloro-benzyloxy substituent in position 4 of the catechol ring, being chemically very similar to the lead compound **2b**, previously resulted active as tubulin polymerization inhibitor.

Subsequently, the cytotoxic activity of the most potent compounds was assessed, on human embryonic fibroblasts (GM-6114) at 10 μM concentration (Table S2, Supporting Material). Interestingly, derivatives **3a** and **4c** did not show any cytotoxicity, whereas compounds **3e**, **5g** and **5h** evidenced some cell growth percent (50, 40.98 and 40.05 % respectively), comparable to most common approved anti-cancer drug as Cis-Pt (39.52 %).

Inhibiting effect on human platelet aggregation and ROS production

Human platelets represent a common cellular element of thrombosis, inflammation, and cancer [25] and can be considered inflammatory cells, due to the release, during platelet activation/aggregation, of inflammatory cytokines, but even increasing the ROS concentration at the level of the vascular damage.[26] Therefore, platelets could be a simple, economic and suitable cellular model based on a causal relationship between inflammation and tumorigenesis.[2,27]

Table 2. Cell growth percent values of imidazo-pyrazoles **3-5** and Cis-Pt used as reference compound on different cancer cell lines at 10 μM concentration. For each compound, only cell lines with a growth percent values < 50% are indicated. Data are mean values for three separate experiments. Variation among triplicate samples is less than 10%.

	Cell growth percent (%)												
Cell line	**3a**	**3c**	**3d**	**3e**	**4b**	**4c**	**4d**	**4e**	**5e**	**5f**	**5g**	**5h**	**Cis-Pt**
A459[a]	35.0	16.1	28.6	24.0	-	-	-	34.2	-	-	42.0	24.3	59.09
Hela[b]	34.9	16.7	22.1	31.9	37.5	44.7	41.0	22.4	45.3	-	39.9	33.8	29.33
Hep-G2[c]	50.6	-	42.0	45.4	-	47.7	-	35.2	-	48.3	42.1	40.0	38.07
MCF7[d]	34.0	17.4	23.3	49.9	-	-	-	27.9	-	-	33.6	-	72.74
MDA-MB321[d]	33.3	35.4	49.7	42.4	-	-	-	39.5	-	-	31.8	26.0	86.07
SK-BR3[d]	-	40.8	37.5	49.1	-	-	-	46.8	-	-	-	-	70.59
SK-Mel28[e]	47.3	24.1	34.4	38.7	-	46.7	-	40.4	42.9	-	44.3	43.5	44.40
SKOV-3[f]	45.4	19.8	32.7	28.6				37.4				39.9	36.83

[a] Lung carcinoma. [b] Cervix epithelioid carcinoma. [c] Hepatocellular carcinoma. [d] Breast cancer. [e] Cutaneous melanoma. [f] Ovarian adenocarcinoma.

Table 3. IC_{50} values of compounds **3a**, **3e**, **4c**, **5g** and **5h** on selected cancer cell lines. Data are the mean ± SD of three experiments.

	IC_{50} (μM) ± SD[g]				
Cell line	**3a**	**3e**	**4c**	**5g**	**5h**
A459[a]	6.71±0.13	2.74±0.38	-	-	2.57±0.27
Hela[b]	6.30± 0.59	4.72±0.06	30.16±3.64	21.67±0.56	6.30±0.59
Hep-G2[c]	7.81±1.24	-	21.49±0.61	-	7.10±0.12
MCF7[d]	7.57±0.37	7.37±1.10	-	22.01±1.83	7.67±0.54
MDA-MB321[d]	6.76±0.28	6.34±0.60	-	19.38±0.89	5.07±0.29
SK-BR3[d]	11.49±0.66	-	-	-	9.04±0.28
SK-Mel28[e]	5.49±0.48	3.08±0.10	30.60±1.72	18.28±0.92	4.94±0.41
SKOV-3[f]	7.36±0.28	2.95±1.03	-	-	6.41±0.28

[a] Lung carcinoma. [b] Cervix epithelioid carcinoma. [c] Hepatocellular carcinoma. [d] Breast cancer. [e] Cutaneous melanoma. [f] Ovarian adenocarcinoma

As previous imidazo-pyrazoles **2** blocked ROS production in platelet and to confirm anti-inflammatory activity of imidazo-pyrazole core already reported,[16,17] the inhibition of platelet aggregation and ROS production on human platelets were evaluated for the most active compounds **3a**, **3e**, **4c**, **5g** and **5h.** As reported in Table 4, compounds **3a** and **4c** showed the lower IC_{50} values for platelet aggregation and ROS production inhibition, suggesting that the shift of the acylhydrazonic substituent from position 7 to position 6 (derivatives **5g**,**h**) or the insertion of bulky substituents on the catechol ring (derivative **3e**) have a detrimental effect on this activity. This specific trend agrees with previous results regarding compounds **2**, where more embedded **2a** and **2b** (more similar to **3e**, **5g** and **5h**) resulted less active as ROS production inhibitors than **2c**, characterized by a smaller substituent on para position of catechol moiety.

Table 4. Inhibitory effect of new synthesized compounds **3a**, **3e**, **4c**, **5g**, **5h** on platelet aggregation and ROS production on human. Reported data are the mean +/- SD obtained in six different experiments each performed in duplicate.

	IC$_{50}$ (μM)) ± SD	
Compound	Aggregation Inhibition	ROS production Inhibition
3a	85.20±6.30	83.00±22.40
3e	160.45±10.42	179.24±33.67
4c	83.89±3.36	74.86±6.18
5g	146.99±19.27	173.22±8.37
5h	140.57±15.85	154.33±0.38

Pharmacokinetic properties and druglikness prediction

To evaluate the pharmaceutical relevance of the most active compounds, the pharmacokinetics and drug-likeness properties of derivatives **3a**, **3e**, **4c**, **5g**, **5h** were calculated by SwissADME (Table S3, Supporting Material).[28] Collectively the considered compounds are characterized by nine rotatable bonds, five to seven H-bond acceptors, two H-bond donors and TPSA values of 89.77 Å^2, thus supporting a good capacity of all derivatives to permeate lipophilic barriers. In addition, all tested imidazo-pyrazoles were predicted to be well absorbed in gastrointestinal (GI) tract and are not expected to pass the brain-blood barrier (BBB); except **4c** and **5h**, they are moderately soluble in water.[29] Derivatives **3a**, **3e**, **4c**, **5g**, **5h** would inhibit 2C19, 2C9, 2D6 and 3A4 cytochromes, without interacting with 1A2 isoform. A Lipinski violation (MW > 500 Da) was identified for compounds **3e**, **4c** and **5h**, but none of the compounds showed any pan assay interference compound (PAINS) alert. Finally, the presence of a C=N functionality was identified as a limitation, according to the Brenk filter.[30]

Docking studies

As previous compounds **2** (particularly **2a** and **2b**) interfere with tubulin system,[16] the ability of new imidazo-pyrazoles **3e** and **5h** (close analogues of **2a** and **2b**) to bind the colchicine binding site in the polymeric complex tubulin α/tubulin β/stathmin4 (PDB ID: 6XER)[31] was evaluated by docking simulations (AutoDock 4.2).[32] Both enantiomers of the two selected ligands were considered, whereas the stereochemistry of the hydrazone CH=N group was kept fixed in the *E* conformation, as assessed by NMR study.

Thus, in the *S*-**3e**/tubulin docking complex (calculated Ki = 2.29 μM), the ligand would assume an extended conformation with the 4-chlorobenzyloxy portion located at equivalent position of the cyclohepta-2,4,6-trien-1-one moiety of colchicine (Figure 3a) and interacting with Lys350, Leu253, Asn256 and Met257 side chains. The complex would be mainly stabilized by two hydrogen bonds involving Thr351 backbone carbonyl and the imidazo-pyrazole and the carbohydrazide NH groups (Figure 3b). Furthermore, ring A (Figure 3b) would establish van der Waals contacts with Asp327 and the imidazo-pyrazole scaffold would interact with Ser178 (α-tubulin), Met323, Asp327 and Thr351 side chains. The interactions between the acylhydrazone linker and Ser178 (α-tubulin), Gln245, Lys350 and those occurring between ring B (Figure 3b) and Leu246 and Ala314 side chains would provide further stabilization to the complex. Isomer *R*-**3e** would assume a similar orientation within the binding site; however, the inversion of the stereocenter would affect the orientation of the imidazo-pyrazole portion and would prevent its ability to form a hydrogen bond with Thr351 (Figure 3c). The calculated Ki value for the *R*-**3e**/tubulin complex was 3.06 μM suggesting a decrease in affinity.

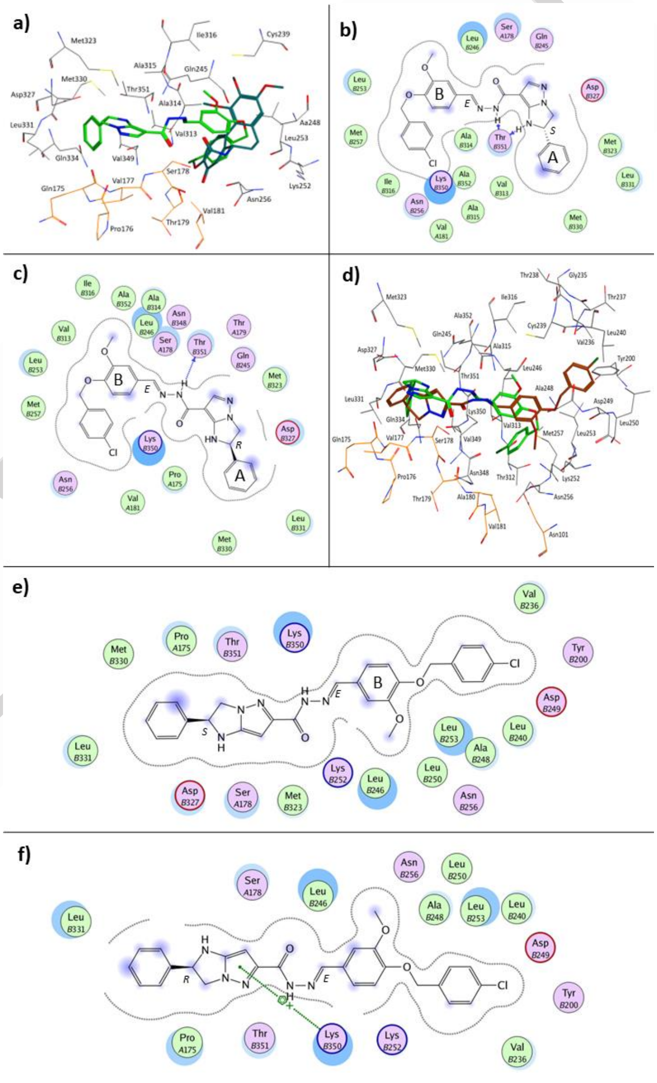

Figure 3. a) Superposition of the binding mode of *S*-**3e** (docking pose, green) and colchicine (X-ray structure, dark green). α- and β-Tubulin residues are coloured orange and grey, respectively. **b)** Ligplot of *S*-**3e**/tubulin complex. **c)** Ligplot of *R*-**3e**/tubulin complex. **d)** Superposition of the docking poses of *S*-**3e** (green) and *S*-**5h** (brown). α- and β-Tubulin residues are coloured orange and grey, respectively. **e)** Ligplot of *R*-**5h**/tubulin complex. **f)** Ligplot of *S*-**5h**/tubulin complex.

The shift of the acylhydrazone substituent from position 7 to position 6 of the imidazo-pyrazole ring would reduce the ability of compounds to bind tubulin. According to docking calculations, the Ki values for *S*-**5h**/tubulin and *R*-**5h**/tubulin complexes were 2- to

5-fold higher than those predicted for their **3e** analogues (Ki$_{(S\text{-}\mathbf{5h})}$ = 12.72 μM; Ki$_{(R\text{-}\mathbf{5h})}$ = 6.23 μM). The bioactive conformations predicted for **5h** enantiomers followed those calculated for isomers **3e**, except for the orientation of the 4-chlorobenzyloxy portion (Figure 3d). In particular, compound *S*-**5h** would adopt an elongated conformation with the 2-phenyl imidazo-pyrazole substructure in contact with Asp327, Leu331, Thr351, Lys350 and Pro175 (α-tubulin) (Figure 3e). The phenyl ring B (Figure 3e) would interact with Leu246, Ala248, Lys252 and Asn256, whereas the 4-chlorobenzyloxy substructure would be in contact with Tyr200, Val236, Leu240, Asp249, Leu250 and Leu253. No hydrogen bond would occur between the ligand and tubulin dimer. In the *R*-**5h**/tubulin docking complex, the imidazo-pyrazole portion would form an arene-cation interaction with Lys350 side chain not observed in the S-**5h**/tubulin complex (Figure 3f).

Molecular dynamics simulation

To further asses the reliability of the docking calculations, a molecular dynamic simulation (explicit solvent, T = 310 K, time = 1 ns) was carried out on the *S*-**3e**/tubulin complex, selected as the most promising docking complex (calculated Ki = 2.29 μM). The analysis of the molecular dynamic trajectory highlighted a stable binding orientation for the ligand with small fluctuations form the docking pose (Figure 4). Furthermore, the analysis of the hydrogen bonding network between *S*-**3e** and tubulin residues (occupancy value percentage) would confirm the interaction between the ligand and Thr351 side chain observed in the *S*-**3e**/tubulin docking complex and would indicate the formation of two additional H-bond with Lys350 and Leu246.

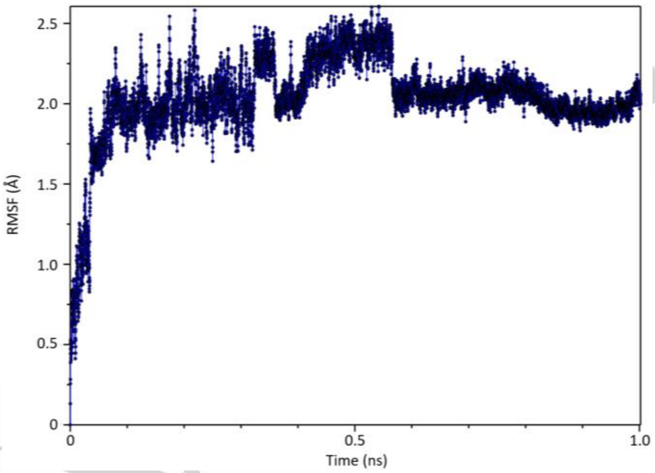

Figure 4. Time dependent root-mean-square fluctuation (RMSF) analysis of ligand *S*-**3e.**

Conclusion

In this paper we investigated the pharmacological properties of imidazo-pyrazole scaffold, not well investigate, to provide important hits useful in medicinal chemistry research and to obtain new pharmacologically active compounds. The SAR extension study on compounds **1** and **2**, allowed the identification of imidazo-pyrazoles **3-5** endowed with significative anti-proliferative and antioxidant properties. Particularly, compounds **3**, more strictly related to lead structures **2a,b**, showed very interesting anti-proliferative activity and collectively the most promising compounds (**3a**, **3e**, **4c**, **5g** and **5h**) resulted no cytotoxic on healthy cells and significantly inhibit ROS production in platelet. In addition, they are endowed with good in silico pharmacokinetics and drug-likeness properties. Finally, molecular docking and molecular dynamic simulations confirmed the possible interaction of most active compounds **3e** and **5h** with tubulin, identified as the biological target for lead derivatives **2a,b**. Collectively, these biological results support the pharmacological potential of this class of derivatives as novel therapeutic agents.

The collected SARs indicate that the anti-proliferative activity is affected by both substitutions on catechol portion and the decoration of imidazo-pyrazole scaffold. Thus, the insertion of an acylhydrazonic moiety at position 6 or 7 led to potent anti-proliferative agents (namely, compounds **3a,e**, **4c**, **5g,h**) whose tumour-specificity is influenced by the substituents of the catechol ring. Compounds bearing bulky substituents (i.e., substituted-benzyloxy and phenoxy) at para position of catechol moiety (as **3e**, **5g** and **5h**), as well as derivatives with the same substituents in meta position (as **3a** and **4c**), provided interesting results. Thus, compounds **3e** and **5g**, sharing the para-clorobenzyloxy moiety, resulted the most effective in conferring a broad spectrum of anti-proliferative activity and showed a potent action particularly against lung carcinoma A459 cell lines, with low micromolar IC$_{50}$ values. On the contrary, the presence of a smaller substituents (phenoxy and difuoromethoxy), as in compounds **3a** and **4c,** resulted in a more specific and selective anti-cancer action and in a great antioxidant potency. In fact, some compounds (i.e., **3e** and **5h**) inhibited the proliferation of several tumor cell lines, while other derivatives (i.e., **4b**, **4d** and **5f**) blocked the growth of specific tumors (namely, HeLa and Hep-G2) worthy of further investigation. On the contrary, as previously observed for derivatives **2**, the antioxidant activity is increased when a poorly hindered substituents (as $OCHF_2$) are present at para position of catechol portion (see derivatives **3a** and **4c**).

All these collected results confirmed that imidazo-pyrazole scaffold linked to a catechol portion differently decorated could represent a valuable moiety for the development of new anti-cancer/anti-inflammatory agents able to act at the intracellular level with different pathways, as ROS production inhibition and tubulin system.[33-35] In particular, derivatives **3** were identified as promising agents endowed with anti-proliferative and antioxidant dual activity. As previously demonstrated, these multiple activities of imidazo-pyrazole chemotype could be partially explained by the close correlation between different intracellular pathways, as tubulin system and ROS production, involved in cancer progression and inflammation.[37,38]

In conclusion, these data may be of interest for the development of future new and more active imidazo-pyrazoles able to interfere with cancer and inflammation with different intracellular mechanisms.

Experimental section

Chemistry

Chiminord and Aldrich Chemical (Milan, Italy) purchased all chemicals. Solvents were reagent grade. All commercial reagents were used without further purification. Aluminium backed silica gel plates (Merck DC-Alufolien Kieselgel 60 F254, Darmstad, Germany), were used in thin-layer chromatography (TLC) for routine monitoring the reaction course. Detection of spots was made by UV light. Merck silica gel, 230–400 mesh, was used for chromatography. Flash chromatography was performed using Isolera one instrument (Biotage, Uppsala, Sweden), using Silicagel column. Melting points are not "corrected" and were measured with a Buchi M-560 instrument (Buchi instruments, Flawil, Switzerland). IR spectra were recorded with a Perkin-Elmer 398 spectrophotometer (Perkin-Elmer, Milan, Italy). ^{1}H and ^{13}C NMR spectra were recorded on JEOL JNM-ECZR (Tokyo, Japan) instrument or a Varian Gemini 200 (200 MHz, Varian Gemini, Palo Alto, CA, USA) using deuterochloroform ($CDCl_3$) or dimethyl sulfoxide (DMSO-d_6) as solvent; chemical shifts are reported as δ (ppm) and signals were characterized as s (singlet), d (doublet), t (triplet), nt (near triplet), q (quartet), m (multiplet), br s (broad signal); J are reported in Hz. IR spectra were recorded with a Perkin- Elmer 398 spectrophotometer (Perkin-Elmer, Milan, Italy).

Elemental analysis was determined with an elemental analyzer EA 1110 (Fison-Instruments, Milan, Italy) and the purity of all synthesized compounds was > 95%; products are considered pure when the difference between calculated and found values is ± than 0.4.

Compounds **8a**,**c, 9a**,**c** and **10a** have been synthesized as previously reported.[7,8,16,17]

Synthesis of 2-hydrazino-1-phenylethanol 7[18]

To $NH_2NH_2\cdot H_2O$ (30 mL, 0.6 mol) at 100 °C, styrene oxide (20 mL, 0.17 mol) is added dropwise, and the mixture is heated at 100 °C for 1 hour.

Then the excess of hydrazine is removed under reduced pressure and the residue is purified by distillation under high vacuum to obtain a colorless liquid used as crude without purification. Molecular formula: $C_8H_{12}N_2O$ (M.W.: 152.19). Yield: 87%. B.p.: 155-158°C/0.6 mmHg.

Synthesis of ethyl 5-amino-1-(2-hydroxy-2-phenylethyl)-3-methyl-1*H*-pyrazole-4-carboxylate 8b.

To 2-cyano-3-ethoxybut-2-enoate [39] (1.2 g, 6 mmol) solved in abs. EtOH (5 mL), 2-hydrazino-1-phenylethanol **10** (0.92 g, 6 mmol) is added and the mixture is heated for 8 hours. After cooling to r.t., solvent is removed under reduced pressure. The brown oil obtained is crystallized from ethyl ether to obtain a white solid. Yield: 57%. M.p.: 123-125 °C. IR ($CHCl_3$): 3440, 3355 (NH_2), 1670 (CO) cm^{-1}. ^{1}H-NMR (200 MHz, $CDCl_3$): δ 1.13 (t, J = 7.0 Hz, 3H, *CH_3*CH_2), 2.40 (s, 3H, CH_3), 3.80-4.38 (m, 4H, CH_2O + CH_2N), 4.93-5.08 (m, 2H, *CH*OH +OH), 5.43 (br s, 2H, NH_2) ,7.02-7.11 (m, 5H, Ar).^{13}C-NMR (101 MHz, DMSO-d_6): δ 162.63, 153.86, 150.94, 142.39, 128.56, 128.19, 127.25, 97.66, 73.02, 60.04, 56.32, 14.93, 14.25. Elemental Analysis calculated for $C_{15}H_{19}N_3O_3$.

Synthesis of ethyl 6-methyl-2-phenyl-2,3-dihydro-1*H*-imidazo[1,2-*b*]pyrazole-7-carboxylate 9b.

Compound **8b** (2.9 g, 10 mmol) is solved in conc. H_2SO_4(10 mL) at 0 °C and the mixture is stirred at r.t. for 15 minutes. Then, iced H_2O (500 mL) is added and the solution is made neutral with conc. NH_4OH solution; the white solid obtained is filtered, washed with H_2O and recrystallized from abs. EtOH. Yield: 80%. M.p.: 140-141.5 °C. IR (KBr): 3333 (NH), 1661 (CO) cm^{-1}. ^{1}H-NMR (200 MHz, $CDCl_3$): δ 1.21-1.43 (m, 3H, *CH_3*CH_2), 2.44 (s, 3H, CH_3), 3.87-4.03 (nt, 1H, H3), 4.16-4.37 (m, 2H, CH_3*CH_2*), 4.43-4.60 (nt, 1H, H3), 5.00 (br, 1H, NH disappear with D_2O), 5.33-5.47 (m, 1H, H2), 7.24-7.51 (m, 5H, Ar). ^{13}C-NMR (101 MHz, $CDCl_3$): 162.08, 157.17, 151.37, 140.65, 128.58, 127.72, 126.02, 92.36, 67.37, 60.04, 57.85, 15.14, 14.25. Elemental Analysis calculated for $C_{15}H_{17}N_3O_2$.

General procedure for synthesis of compounds 10a-c.

Compounds **9a-c** (15 mmol) and $NH_2NH_2\cdot H_2O$ (14 mL, 750 mg, 16 mmol) are heated to 120-130 °C for 3 hours. After cooling to r.t., H_2O (50 mL) is added and the white solid obtained is filtered, washed several times with H_2O and recrystallized from 95% EtOH.

*6-Methyl-2-phenyl-2,3-dihydro-1H-imidazo[1,2-b]pyrazole-7-carbohydrazide (**10b**).* Yield: 51%. M.p.: 231-232 °C. ^{1}H-NMR (400 MHz, DMSO-d_6): 2.27 (s, 3H, CH_3), 3.70 (nt, 1H, H3), 4.23 (br s, 2H, NH_2 disappears with D_2O), 4.49 (nt, 1H, H3), 5.36 (nt, 1H, H2), 6.99 (br s, 1H, NH disappears with D_2O), 7.31-7.44 (m, 5H, Ar), 8.11 (s, 1H, CONH, disappears with D_2O). ^{13}C-NMR (101 MHz, DMSO-d_6): δ 166.61, 157.30, 146.65, 140.79, 128.58, 127.72, 126.02, 90.02, 67.34, 58.00, 15.13. Elemental Analysis calculated for $C_{13}H_{15}N_5O$.

*2-Phenyl-2,3-dihydro-1H-imidazo[1,2-b]pyrazole-6-carbohydrazide (**10c**).* Yield:76%. M.p.199-200 °C. ^{1}H-NMR (400 Mz, DMSO-d_6): 3.81 (nt, 1H, H3), 4.31 (br s, 2H, NH_2, disappears with D_2O), 4.60 (nt, 1H, H3), 5.35 (nt, 1H, H2), 5.67 (s, 1H, H7), 6.57 (s, 1H, NH, disappears with D_2O), 7.30-7.45 (m, 5H, Ar), 9.13 (s, 1H, CONH, disappears with D_2O). ^{13}C-NMR (101 MHz, DMSO-d_6): δ 162.85, 154.75, 146.27, 140.17, 128.58, 127.72, 126.02, 82.04, 67.85, 56.63. Elemental Analysis calculated for $C_{12}H_{13}N_5O$.

General procedure for synthesis of compounds 3-5.

To a solution of carbohydrazide **10a-c** (1 mmol) in abs. EtOH (10 mL) the suitable aldehyde **6a-g** (1 mmol) solved in abs. EtOH (2 mL) is added dropwise. The reaction mixture is heated at reflux for 1-18 hours. After cooling to room temperature, the solvent is removed under reduced pressure to obtain yellow/white solids which are filtered and re-crystallized from abs. EtOH or ethyl acetate.

*(E)-N'-(4-(difluoromethoxy)-3-phenoxybenzylidene)-2-phenyl-2,3-dihydro-1H-imidazo[1,2-b]pyrazole-7-carbohydrazide (**3a**).* M.p: 99-100 °C (abs. ethanol). ^{1}H-NMR (200 MHz, DMSO-d_6): δ

3.75 (nt, 1H, H3), 4.55 (nt, 1H, H3), 5.38 (nt, 1H, H2), 6.93-7.80 (m, 15H, 10Ar + H-5 Ar + H-6 Ar + H-2 Ar + $OCHF_2$ + H6), 8.00 (br s, 1H, CH=N), 11.14 (s, 1H, NH disappears with D_2O). ^{13}C-NMR (100 MHz, DMSO-d_6): δ 160.08, 156.83, 153.01, 147.67, 145.13, 144.77,1-37.24, 130.02, 128.58, 128.30, 127.72, 126.02, 124.60, 122.31, 118.78, 115.76, 114.87, 113.66, 95.14, 67.31, 57.64. Elemental Analysis calculated for $C_{26}H_{21}F_2N_5O_3$.

(E)-N'-(3-(benzyloxy)-4-(difluoromethoxy)benzylidene)-2-phenyl-2,3-dihydro-1H-imidazo[1,2-b]pyrazole-7-carbohydrazide ***(3b)****.* M.p: 134-135 °C (ethyl acetate). ^{1}H-NMR (400 MHz, DMSO-d_6): δ 3.82 (nt, 1H, H3), 4.62 (nt, 1H, H3), 5.43 (m, 2H, CH_2O), 5.46 (nt, 1H, H2), 6.97-7.68 (m, 15H, 10Ar + H-5 Ar + H-6 Ar + H-2 Ar + $OCHF_2$ + H6), 7.94 (s, 1H, CH=N), 11.19 (s, 1H, NH disappears with D_2O). ^{13}C-NMR (101 MHz, DMSO-d_6): δ 160.08, 153.01, 150.58, 144.67, 140.79, 137.49, 128.56, 128.49, 128.20, 128.15, 127.72, 126.02, 122.14, 118.96, 117.87, 115.77, 113.66, 111.68, 95.14, 71.24, 67.31, 57.64. Elemental Analysis calculated for $C_{27}H_{23}F_2N_5O_3$.

(E)-N'-(4-((4-fluorobenzyl)oxy)-3-methoxybenzylidene)-2-phenyl-2,3-dihydro-1H-imidazo[1,2-b]pyrazole-7-carbohydrazide ***(3c)****.* M.p: 119-120 °C (abs. ethanol). ^{1}H-NMR (400 MHz, DMSO-d_6): δ 3.79-3.84 (m, 4H, OCH_3 + H3), 4.61 (nt, 1H, H3), 5.11 (s, 2H, CH_2O), 5.45 (nt, 1H, H2), 7.08-7.52 (m, 13H, 10Ar + H-5 Ar + H-6 Ar + H-2 Ar + H6), 7.98 (br s, 1H, CH=N), 11.06 (br s, 1H, CONH, disappears with D_2O). ^{13}C-NMR (101 MHz, DMSO-d_6): δ 163.56, 161.59, 160.08, 153.01, 150.54, 144.53, 140.79, 137.24, 133.38, 130.14, 130.07, 128.58, 127.72, 126.02, 121.64, 115.46, 115.28, 114.35, 109.98, 95.14, 71.29, 67.31, 57.64, 56.02. Elemental Analysis calculated for $C_{27}H_{24}FN_5O_3$.

(E)-N'-(4-((3-fluorobenzyl)oxy)-3-methoxybenzylidene)-2-phenyl-2,3-dihydro-1H-imidazo[1,2-b]pyrazole-7-carbohydrazide ***(3d)****.* M.p: 191-192 °C (abs. ethanol).^{1}H-NMR (400 MHz, DMSO-d_6): δ 3.79-3.85 (m, 4H, OCH_3 +H3), 4.61 (nt, 1H, H3), 5.16 (s, 2H, CH_2O), 5.45 (nt, 1H, H2), 7.07-7.48 (m, 13H, 9Ar + H-5 Ar + H-6 Ar + H-2 Ar + H6), 7.98 (br s, 1H, CH=N), 11.07 (br s, 1H, CONH, disappears with D_2O). ^{13}C-NMR (101 MHz, DMSO-d_6): δ 162.51, 160.54, 153.01, 150.57, 144.53, 140.79, 138.05, 137.24, 130.01, 129.93, 128.58, 127.72, 126.02, 122.98, 121.64, 114.37, 114.18, 114.05, 113.87, 109.96, 95.14, 70.46, 67.31, 57.64, 56.02. Elemental Analysis calculated for $C_{27}H_{24}FN_5O_3$.

(E)-N'-(4-((4-chlorobenzyl)oxy)-3-methoxybenzylidene)-2-phenyl-2,3-dihydro-1H-imidazo[1,2-b]pyrazole-7-carbohydrazide ***(3e)****.* M.p: 118-119 °C (abs. ethanol). ^{1}H-NMR (400 MHz, DMSO-d_6): δ 3.79-4.07 (m, 4H, OCH_3 + H3), 4.61 (nt, 1H, H3), 5.13 (s, 2H, OCH_2), 5.45 (nt, 1H, H2), 7.06-7.50 (m, 13H, 9Ar + H-5 Ar + H-6 Ar + H-2 Ar + H6), 7.98 (br s, 1H, CH=N), 11.06 (br s, 1H, CONH, disappears with D_2O). ^{13}C-NMR (101 MHz, DMSO-d_6): δ 160.08, 153.01, 150.54, 144.53, 140.79, 137.24, 135.25, 134.08, 129.75, 128.64, 128.58, 127.72, 126.02, 121.64, 114.35, 109.98, 95.14, 71.29, 67.31, 57.64, 56.02. Elemental Analysis calculated for $C_{27}H_{24}ClN_5O_3$.

(E)-N'-(3-(cyclopentyloxy)-4-methoxybenzylidene)-6-methyl-2-phenyl-2,3-dihydro-1H-imidazo[1,2-b]pyrazole-7-carbohydrazide ***(4a)****.* M.p: 151-152 °C (abs. ethanol). ^{1}H-NMR (400 MHz, DMSO-d_6): δ 1.46-1.68 (m, 8H, 4CH_2 cyclopent.), 2.47 (s, 3H, CH_3), 4.04-4.08 (m, 4H, OCH_3 + H3), 4.52 (nt, 1H, H3), 4.84-4.85 (m, 1H, CHO cyclopent.), 5.27 (nt, 1H, H2), 5.51 (br s, 1H, NH, disappears with D_2O), 6.99 (d, J = 8 Hz, 1H, H-5 Ar), 7.10 (d, J = 8 Hz, 1H, H-6 Ar), 7.18 -7.54 (m, 6H, 5 Ar + H-2 Ar), 7.97 (s, 1H, CH=N), 11.07 (br s, 1H, CONH, disappears with D_2O). ^{13}C-NMR (101 MHz, DMSO-d_6): δ 160.35, 152.32, 151.83, 147.74, 145.85, 144.57, 140.79, 128.58, 128.06, 127.72, 126.02, 124.23, 113.06, 112.85, 91.10, 80.51, 67.34, 58.00, 56.09, 32.81, 23.45, 15.11. Elemental Analysis calculated for $C_{26}H_{29}N_5O_3$.

(E)-N'-(3-(cyclopentyloxy)-4-(difluoromethoxy)benzylidene)-6-methyl-2-phenyl-2,3-dihydro-1H-imidazo[1,2-b]pyrazole-7-carbohydrazide ***(4b)****.* M.p: 110-111 °C (abs. ethanol). ^{1}H-NMR (400 MHz, DMSO-d_6): δ 1.59-1.97 (m, 8H, 4CH_2 cyclopent.), 2.46 (s, 3H, CH_3), 3.81 (nt, 1H, H3), 4.61 (nt, 1H, H3), 4.90-4.93 (m, 1H, CHO cyclopent.), 5.42 (nt, 1H, H2), 7.01 (t, J = 70 Hz, 1H, $OCHF_2$), 7.13-7.42 (m, 8H, 5Ar + H-5 Ar + H-6 Ar + H-2 Ar), 7.99 (br s, 1H, CH=N), 11.17 (br s, 1H, CONH, disappears with D_2O). ^{13}C-NMR (101 MHz, DMSO-d_6): δ 160.35, 152.32, 149.05, 145.85, 145.20, 145.15, 144.67, 140.79, 128.58, 128.00, 127.72, 126.02, 121.92, 119.28, 117.87, 115.77, 113.66, 91.10, 81.11, 67.34, 58.00, 32.81, 23.45, 15.11. Elemental Analysis calculated for $C_{26}H_{27}F_2N_5O_3$.

(E)-N'-(4-(difluoromethoxy)-3-phenoxybenzylidene)-6-methyl-2-phenyl-2,3-dihydro-1H-imidazo[1,2-b]pyrazole-7-carbohydrazide ***(4c)****.* ^{1} M.p: 130-131 °C (ethyl acetate). H-NMR (400 MHz,DMSO-d_6): δ 2.58 (s, 3H, CH_3), 4.20 (nt, 1H, H3), 4.64 (nt, 1H, H3), 5.48 (nt, 1H, H2), 7.01-7.40 (m, 17H, 13Ar + H-5 Ar + H-6 Ar + H-2 Ar + $OCHF_2$), 8.03 (s, 1H, CH=N), 11.16 (br s, 1H, CONH, disappears with D_2O). ^{13}C-NMR (101 MHz, DMSO-d_6): δ 160.35, 156.83, 152.32, 147.66, 145.85, 145.08, 144.77, 140.79, 130.02, 128.58, 128.30, 127.72, 126.02, 124.60, 122.31, 118.76, 117.87, 115.76, 114.87, 113.66, 91.10, 67.34, 58.00, 15.11. Elemental Analysis calculated for $C_{27}H_{23}F_2N_5O_3$.

(E)-N'-(3-(benzyloxy)-4-(difluoromethoxy)benzylidene)-6-methyl-2-phenyl-2,3-dihydro-1H-imidazo[1,2-b]pyrazole-7-carbohydrazide ***(4d)****.* M.p: 129-131 °C (ethyl acetate). ^{1}H-NMR (400 MHz,DMSO-d_6): δ 2.46 (s, 3H, CH_3), 3.79 (nt, 1H, H3), 4.59 (nt, 1H, H3), 5.20 (s, 2H, OCH_2), 5.42 (nt, 1H, H2), 6.93-7.46 (m, 14H, 10Ar + H-5 Ar + H-6 Ar + H-2 Ar + $OCHF_2$), 7.91 (br s, 1H, CH=N), 11.15 (br s, 1H, CONH, disappears with D_2O). ^{13}C-NMR (101 MHz, DMSO-d_6): δ 160.35, 152.32, 150.56, 145.85, 144.54, 140.79, 137.49, 128.58, 128.22, 128.16, 127.72, 126.02, 122.14, 118.98, 117.87, 115.77, 113.66, 111.68, 91.10, 71.24, 67.34, 58.00, 15.11. Elemental Analysis calculated for $C_{28}H_{25}F_2N_5O_3$.

(E)-N'-(4-((4-fluorobenzyl)oxy)-3-methoxybenzylidene)-6-methyl-2-phenyl-2,3-dihydro-1H-imidazo[1,2-b]pyrazole-7-carbohydrazide ***(4e)****.* M.p: 78-80 °C (abs. ethanol). ^{1}H-NMR (400 MHz DMSO-d_6): δ 2.47 (s, 3H, CH_3), 3.32 (s, 3H, OCH_3), 3.86 (nt, 1H, H3), 4.45 (nt, 1H, H3), 5.05 (br s, 1H, NH disappears with D_2O), 5.10 (s, 2H, OCH_2), 5.49 (nt, 1H, H2), 7.22-7.55 (m, 12H, 9Ar + H-5 Ar + H-6 Ar + H-2 Ar), 8.63 (s, 1H, CH=N), 11.19 (br s, 1H, CONH, disappears with D_2O). ^{13}C-NMR (101 MHz, DMSO-d_6): δ 163.56, 161.59, 160.35, 152.32, 150.54, 145.85, 144.53, 140.79, 133.38, 130.14, 130.07, 128.58, 127.72, 126.02, 121.64,

115.46, 115.28, 114.35, 109.98, 91.10, 71.29, 67.34, 58.00, 56.02, 15.11. Elemental Analysis calculated for $C_{28}H_{26}FN_5O_3$.

*(E)-N'-(4-((3-fluorobenzyl)oxy)-3-methoxybenzylidene)-6-methyl-2-phenyl-2,3-dihydro-1H-imidazo[1,2-b]pyrazole-7-carbohydrazide **(4f)***. M.p: 98-99 °C (abs. ethanol). ^{1}H-NMR (400 MHz,DMSO-d_6): δ 2.47 (s, 3H, CH_3), 3.41 (s, 3H, OCH_3), 3.76 (nt, 1H, H3), 4.45 (nt, 1H, H3), 5.07 (s, 2H, OCH_2), 5.35 (nt, 1H, H2), 5.44 (br s, 1H, NH disappears with D_2O), 6.92-7.40 (m, 12H, 9Ar + H-5 Ar + H-6 Ar + H-2 Ar), 8.14 (s, 1H, CH=N), 11.19 (br s, 1H, CONH, disappears with D_2O). ^{13}C-NMR (101 MHz, DMSO-d_6): δ 162.51, 160.54, 160.35, 152.32, 150.57, 145.85, 144.53, 140.79, 138.05, 137.99, 130.01, 129.93, 128.58, 127.72, 126.02, 122.95, 121.64, 114.37, 114.18, 113.87, 109.96, 91.10, 70.46, 67.34, 58.00, 56.02, 15.11. Elemental Analysis calculated for $C_{28}H_{26}FN_5O_3$.

*(E)-N'-(4-((4-chlorobenzyl)oxy)-3-methoxybenzylidene)-6-methyl-2-phenyl-2,3-dihydro-1H-imidazo[1,2-b]pyrazole-7-carbohydrazide **(4g)***. M.p: 91-92 °C (abs. ethanol). ^{1}H-NMR (400 MHz,DMSO-d_6): δ 2.47 (s, 3H, CH_3), 3.46 (s, 3H, OCH_3), 3.73 (nt, 1H, H3), 4.46 (nt, 1H, H3), 5.07 (s, 2H, OCH_2), 5.27-5.30 (m, 2H, H2 + NH, 1H disappears with D_2O), 7.17-7.50 (m, 12H, 9Ar + H-5 Ar + H-6 Ar + H-2 Ar), 8.01 (s, 1H, CH=N), 11.19 (br s, 1H, CONH, disappears with D_2O). ^{13}C-NMR (101 MHz, DMSO-d_6): δ 160.35, 152.32, 150.54, 145.85, 144.53, 140.79, 135.25, 134.08, 129.75, 128.64, 128.58, 127.72, 126.02, 121.64, 114.35, 109.98, 91.10, 71.29, 67.34, 58.00, 56.02, 15.11. Elemental Analysis calculated for $C_{28}H_{26}ClN_5O_3$.

*(E)-N'-(3-(cyclopentyloxy)-4-methoxybenzylidene)-2-phenyl-2,3-dihydro-1H-imidazo[1,2-b]pyrazole-6-carbohydrazide **(5a)***. M.p: 174-175 °C (ethyl acetate). ^{1}H-NMR (400 MHz,DMSO-d_6): δ 1.64-1.69 (m, 8H, 4CH_2 cyclopent.), 3.85 (s, 3H, OCH_3), 3.87 (nt, 1H, H3), 4.64 (nt, 1H, H3), 4.65-4.67 (m, 1H, CHO cyclopent.), 5.35 (nt, 1H, H2), 5.77 (s, 1H, H7), 6.62 (s, 1H, NH, disappears with D_2O), 6.99 (d, J = 8 Hz, 1H, H-5 Ar), 7.09 (d, J = 2 Hz, 1H, H-6 Ar), 7.15 (s, 1H, H-2 Ar), 7.26-7.44 (m, 5H, Ar), 8.29 (s, 1H, CH=N), 11.18 (br s, 1H, CONH, disappears with D_2O). ^{13}C-NMR (101 MHz, DMSO-d_6): δ 160.84, 154.76, 151.83, 147.74, 145.70, 144.69, 140.17, 128.58, 128.06, 127.72, 126.02, 124.28, 113.06, 112.85, 83.28, 80.51, 67.86, 56.63, 56.09, 32.81, 23.45. Elemental Analysis calculated for $C_{25}H_{27}N_5O_3$.

*(E)-N'-(3-(cyclopentyloxy)-4-(difluoromethoxy)benzylidene)-2-phenyl-2,3-dihydro-1H-imidazo[1,2-b]pyrazole-6-carbohydrazide **(5b)***. M.p: 145-149 °C (ethyl acetate). ^{1}H-NMR (400 MHz DMSO-d_6): δ 1.50-1.68 (m, 8H, 4CH_2 cyclopent.), 3.96 (nt, 1H, H3), 4.48 (nt, 1H, H3), 4.88-4.90 (m, 1H, CHO cyclopent.), 5.31 (nt, 1H, H2), 5.73 (s, 1H, H7), 6.75 (br s, 1H, NH, disappears with D_2O), 7.22 (t, J = 70 Hz, 1H, $OCHF_2$), 7.26-7.38 (m, 8H, H-5 Ar + H-6 Ar + H-2 Ar + 5Ar), 7.94 (s, 1H, CH=N), 11.18 (br s, 1H, CONH, disappears with D_2O). ^{13}C-NMR (101 MHz, DMSO-d_6): δ 160.84, 154.76, 149.03, 145.70, 145.15, 144.66, 140.17, 128.58, 127.96, 127.72, 126.02, 121.95, 119.30, 119.28, 117.87, 115.77, 113.66, 112.99, 83.28, 81.11, 67.86, 56.63, 32.81, 23.45. Elemental Analysis calculated for $C_{25}H_{25}F_2N_5O_3$.

*(E)-N'-(4-(difluoromethoxy)-3-phenoxybenzylidene)-2-phenyl-2,3-dihydro-1H-imidazo[1,2-b]pyrazole-6-carbohydrazide **(5c)***. M.p: 168-169 °C (ethyl acetate). ^{1}H-NMR (200 MHz,DMSO-d_6): δ 3.51 (br s, 1H, NH, disappears with D_2O), 3.84 (nt, 1H, H3), 4.60 (nt, 1H, H3), 5.39 (nt, 1H, H2), 5.82 (s, 1H, H7), 6.98-7.40 (m, 14H, 10Ar + H-5 Ar + H-6 Ar + H-2 Ar + $OCHF_2$), 8.69 (s, 1H, CH=N), 11.18 (br s, 1H, CONH, disappears with D_2O). ^{13}C-NMR (101 MHz, DMSO-d_6): δ 160.84, 156.83, 154.76, 147.66, 145.70, 145.08, 144.66, 140.17, 130.02, 128.58, 128.32, 127.72, 126.02, 124.60, 122.31, 118.78, 117.87, 115.76, 114.87, 113.66, 83.28, 67.86, 56.63. Elemental Analysis calculated for $C_{26}H_{21}F_2N_5O_3$.

*(E)-N'-(3-(benzyloxy)-4-(difluoromethoxy)benzylidene)-2-phenyl-2,3-dihydro-1H-imidazo[1,2-b]pyrazole-6-carbohydrazide **(5d)***. M.p: 96-98 °C (abs. ethanol). ^{1}H-NMR (200 MHz,DMSO-d_6): δ 3.90 (nt, 1H, H3), 4.70 (nt, 1H, H3), 5.22 (s, 2H, OCH_2), 5.42 (nt, 1H, H2), 5.73 (s, 1H, H7), 6.70 (br s, 1H, NH, disappears with D_2O), 7.11-7.57 (m, 13H, H-5 Ar + H-6 Ar + H-2 Ar + $OCHF_2$ + 9Ar), 8.39 (s, 1H, CH=N), 11.16 (br s, 1H, CONH, disappears with D_2O). ^{13}C-NMR (101 MHz, DMSO-d_6): δ 160.84, 154.76, 150.56, 145.70, 144.66, 144.49, 140.17, 137.49, 128.58, 128.18,-127.72, 126.02, 122.14, 118.98, 117.87, 115.77, 113.66, 111.68, 83.28, 71.24, 67.86, 56.63. Elemental Analysis calculated for $C_{27}H_{23}F_2N_5O_3$.

*(E)-N'-(4-(benzyloxy)-3-methoxybenzylidene)-2-phenyl-2,3-dihydro-1H-imidazo[1,2-b]pyrazole-6-carbohydrazide **(5e)***. M.p: 99-100 °C (ethyl acetate). ^{1}H-NMR (400 MHz, $CDCl_3$): δ 3.81 (s, 3H, OCH_3), 3.87 (nt, 1H, H3), 4.68 (nt, 1H, H3), 5.10 (s, 2H, OCH_2), 5.36 (nt, 1H, H2), 5.75 (s, 1H, H7), 6.68 (br s, 1H, NH, disappears with D2O), 7.02-7.49 (m, 12H, 9Ar + H-5 Ar + H-6 Ar + H-2 Ar), 8.36 (s, 1H, CH=N), 11.45 (br s, 1H, CONH, disappears with D_2O).^{13}C-NMR (101 MHz, DMSO-d_6): δ 160.84, 154.76, 150.54, 150.52, 145.70, 144.69, 140.17, 136.03, 128.58, 128.16, 127.85, 127.72, 127.71, 126.02, 121.64, 114.35, 109.98, 83.28, 71.06, 67.86, 56.63, 56.02. Elemental Analysis calculated for $C_{27}H_{24}N_5O_3$.

*(E)-N'-(3-((4-fluorobenzyl)oxy)-4-methoxybenzylidene)-2-phenyl-2,3-dihydro-1H-imidazo[1,2-b]pyrazole-6-carbohydrazide **(5f)***. M.p: 175-176 °C (abs. ethanol). ^{1}H-NMR (400 MHz, DMSO-d_6): δ 3.79 (s, 3H, OCH_3), 3.87 (nt, 1H, H3), 4.62 (nt, 1H, H3), 5.06 (s, 2H, OCH_2), 5.32 (nt, 1H, H2), 5.73 (s, 1H, H7), 6.59 (br s, 1H, NH, disappears with D_2O), 7.03-7.55 (m, 12H, 9Ar + H-5 Ar + H-6 Ar + H-2 Ar), 8.38 (s, 1H, CH=N), 11.18 (br s, 1H, CONH, disappears with D_2O). ^{13}C-NMR (101 MHz, DMSO-d_6): δ 163.56, 161.59, 160.84, 154.76, 150.54, 145.70, 144.69, 140.17, 133.38, 130.14, 130.07, 128.58, 127.85, 127.72, 126.02, 121.64, 115.46, 115.28, 114.35, 109.98, 83.28, 71.29, 67.86, 56.63, 56.02. Elemental Analysis calculated for $C_{27}H_{24}FN_5O_3$.

*(E)-N'-(3-((3-fluorobenzyl)oxy)-4-methoxybenzylidene)-2-phenyl-2,3-dihydro-1H-imidazo[1,2-b]pyrazole-6-carbohydrazide **(5g)***. M.p: 193-194 °C (abs. ethanol). ^{1}H-NMR (400 MHz,DMSO-d_6): δ 3.80 (s, 3H, OCH_3), 3.90 (nt, 1H, H3), 4.66 (nt, 1H, H3), 5.06 (s, 2H, OCH_2), 5.35 (nt, 1H, H2), 5.70 (s, 1H, H7), 6.61 (br s, 1H, NH, disappears with D_2O), 7.03-7.41 (m, 12H, 9Ar + H-5 Ar + H-6 Ar + H-2 Ar), 8.30 (s, 1H, CH=N), 11.18 (br s, 1H, CONH, disappears with D_2O). ^{13}C-NMR (101 MHz, DMSO-d_6): δ 162.51, 160.84, 154.76, 150.57, 145.70, 144.69, 140.17, 138.05, 130.01, 129.93, 128.58, 127.85, 126.02, 122.98, 121.65, 114.37, 114.18, 114.05,

113.87, 109.96, 83.28, 70.46, 70.43, 67.86, 56.63, 56.02. Elemental Analysis calculated for $C_{27}H_{24}FN_5O_3$.

(E)-N'-(3-((4-chlorobenzyl)oxy)-4-methoxybenzylidene)-2-phenyl-2,3-dihydro-1H-imidazo[1,2-b]pyrazole-6-carbohydrazide ***(5h)****.* M.p: 204-205 °C (abs. ethanol). ^{1}H-NMR (400 MHz,DMSO-d_6): δ 3.76 (s, 3H, OCH_3), 3.85 (nt, 1H, H3), 4.59 (nt, 1H, H3), 5.07 (s, 2H, OCH_2), 5.39 (nt, 1H, H2), 5.74 (s, 1H, H7), 6.62 (br s, 1H, NH, disappears with D_2O), 6.97-7.53 (m, 12H, 9Ar + H-5 Ar + H-6 Ar + H-2 Ar), 8.27 (s, 1H, CH=N), 11.18 (br s, 1H, CONH, disappears with D2O). ^{13}C-NMR (101 MHz, DMSO-d_6): δ 160.84, 154.76, 150.54, 145.70, 144.69, 140.17, 135.25, 134.08, 129.75, 128.64, 128.58,127.85, 127.72, 126.02, 121.64, 114.35, 109.98, 83.28, 71.29, 67.86, 56.63, 56.02. Elemental Analysis calculated for $C_{27}H_{24}ClN_5O_3$.

Anti-proliferative activity

To perform MTT assay, SK-BR3 (breast andenocarcinoma, Biologic Bank and Cell Factory, IRCCS Policlinico San Martino, Genoa, Italy), MCF-7 (breast adenocarcinoma, Biologic Bank and Cell Factory, IRCCS Policlinico San Martino, Genoa, Italy), SK-Mel28 (skin melanoma, Biologic Bank and Cell Factory, IRCCS Policlinico San Martino, Genoa, Italy), Hep-G2 (hepatocellular carcinoma, ATCC, Manassas, VA), SKOV-3 (ovarian adenocarcinoma, ATCC, Manassas, VA), MDA-MB231 (breast adenocarcinoma, Biologic Bank and Cell Factory, IRCCS Policlinico San Martino, Genoa, Italy), HeLa (cervical adenocarcinoma, Biologic Bank and Cell Factory, IRCCS Policlinico San Martino, Genoa, Italy), A549 (lung carcinoma, Biologic Bank and Cell Factory, IRCCS Policlinico San Martino, Genoa, Italy) and GM-6114 (embryonic human fibroblast, ATCC, Manassas, VA) cell lines were cultured in Dulbecco's Modified Eagle Medium (DMEM), added with 10% Fetal bovine serum (FBS), 2 mM Glutamine and 1% penstrep. Reagents were acquired from EuroClone (Milan, Italy) and incubated in a humidified environment at 37 °C with 5% CO_2. All chemical compounds were dissolved in DMSO to give a 10 mM stock solution. Then, after an intermediate dilution in growth medium, they were added to the cultured cells at a final working concentration of 10 μM (1, 5, 10 μM for IC_{50} assay) and incubated for 48 hours. At the end of the incubation, 30 μL of MTT (3-(4,5-dimethyl-2-thiazolyl)-2,5-diphenyl-2H-tetrazolium bromide) at a concentration of 2 mg/mL in phosphate buffered saline (PBS), were added in each well and incubated 4 hours. Finally, the supernatants were removed and 100 μL/well of DMSO were added to each well to dissolve the Formazan precipitates. After 20 min, the results were read at 570 nm. Results are expressed as percentage of the control samples, where cells have been treated with the same amount of DMSO but without any chemical compound. The assay was repeated three times and a single compound was tested six times. Means and standard deviations were calculated.

The IC_{50} values were calculated based on single concentration-response curves. Each experiment was repeated three times.

Blood Collection and Preparative Procedures

Freshly drawn venous blood from healthy volunteers of the "Centro Trasfusionale, Ospedale San Martino" in Genoa was collected into 130 mM aqueous trisodium citrate anticoagulant solution (9:1). The donors claimed to have not taken drugs known to interfere with platelet function during two weeks prior to blood collection and gave their in-formed consent. Washed platelets were prepared centrifuging whole blood at 100×g for 20 min. The obtained platelet-rich plasma was then centrifuged at 1100×g for 15 min. Pellet was washed once with pH 5.2 ACD solution (75 mM trisodium citrate, 42 mM citric acid and 136 mM glucose), centrifuged at 1100×g for 15 min and then resuspended in pH 7.4 Hepes buffer (145 mM NaCl, 5 mM KCl, 1 mM MgSO4, 10 mM glucose, 10 mM HEPES).

The reported IC_{50} values are the molar concentration of the compound able to obtain 50% inhibition of the maximal effect induced by thrombin (Sigma-Aldrich/Merck Millipore) and are calculated by the percentage of inhibition that are the inhibition of the maximal effect measured in the presence of the agent compared with that measured in a control sample containing saline, carried out under the same conditions.

ROS Assay

ROS production was quantified as previously reported[9,15] by 2′,7′-Dichlorofluorescein diacetate (DCFH-DA, Sigma-Aldrich/Merck Millipore), a ROS-sensitive probe that yields, upon oxidation, the fluorescent adduct DCF that is trapped in-side the cells. Briefly, washed platelets (1.0×10^8/mL), preincubated with saline and tested compounds for 15 min at 37°C, were stimulated by 0.1 U/mL thrombin. Incubation was stopped by cooling samples in ice bath and then samples were immediately analysed in a Merck Millipore Bioscience Guava easyCyte flow cytometer (Merk Millipore, Burlington, MA, USA). The IC_{50} values were calculated as above detailed.

Platelet Aggregation

Platelet aggregation was performed in a Bio-Data Aggregometer (Bio-Data Corporation, Horsham, PA, USA) according to Born's method [40] and quantified by the light transmission reached within 6 min at 37°C. Briefly, washed platelets (3.0×10^8/mL) were pre-incubated for 3 min at 37°C with saline or tested compounds before the addition of 0.1 U/mL thrombin. The IC_{50} values were calculated as above detailed.

Docking studies

The molecular structures of compounds *R*-**3e**, *S*-**3e**, *R*-**5h** and *S*-**5h** were built by MOE2009.10 (builder module), parameterized by MMFF94x force field and their docking poses within tubulin were calculated by Autodock 4.2.[32] After the removal of water molecules and ligand atoms from the crystal structure of tubulin α/tubulin β/stathmin4 (PDB ID: 6XER),[31] polar hydrogen and Gasteiger-Huckel charges were added. The ligands root was defined automatically. A 60 × 60 × 60 Å grid (grid spacing 0.375 Å) was centred in the binding site of colchicine, and electrostatic and affinity maps for each atom type of the ligand were calculated. The docking search was performed over 100 conformers using the Genetic Algorithm Local Search protocol as implemented in

Autodock (population size: 50; rate of gene mutation: 0.02; rate of crossover: 0.8). The docking poses were clustered (rmsd: 2.0 Å) and the best conformation of the low energy highest populated cluster was selected as the binding conformation. Model analysis was carried out using the CCP4 program suite.[41] The calculations were run on a Linux PC (Intel® processor Core™ i7-2600 CPU@3.40 GHz).

Molecular dynamic studies

The coordinates of *S*-**3e** docking pose were parametrized by CHARMM-GUI.[42] The molecular structure of tubulin dimer was processed and parametrized by VMD package (Automatic PSF building module). [43] The protein-ligand complex was assembled and a solvation box including the whole complex (max box padding: x = 7; y = 7, z = 7) was defined. 15059 water molecules were added, and the complex was neutralized by the addition of NaCl ions.

The molecular dynamic simulation was carried out by software NAMD, developed by the Theoretical and Computational Biophysics Group in the Beckman Institute for Advanced Science and Technology at the University of Illinois at Urbana-Champaign. [44] The following parameter were adopted: run = 501000; time step = 2; temperature = 310; restartfreq = 50. VMD “RMSD trajectory tool” and “Hydrogen bonds” were used to analyse the trajectory file. The calculations were run on a Linux PC (Intel® processor Core™ i7-2600 CPU@3.40 GHz).

Supporting Information

The elemental analysis values, cell growth percent values of compounds **3a**, **3e**, **4c**, **5g** and **5h** on human embryonic fibroblasts (GM-6114) at 10 μM concentration. Predicted pharmacokinetics and drug-like properties of compounds **3a**, **3e**, **4c**, **5g, 5h** and the NMR scans of all compounds **3-5** are provided.

Acknowledgements

The authors thank Dr. M. Anzaldi and R. Raggio for spectral recording and elemental analysis. E.I. was supported by Fondazione Umberto Veronesi.

Keywords: imidazo-pyrazoles • anti-cancer activity • ROS • molecular docking • medicinal chemistry

[1] http: www.cancer.gov/about-cancer/understanding/statistics (accessed 1 May 2023).

[2] N. Singh, D. Baby, J. P. Rajguru, P. B. Patil, S. S. Thakkannavar, V. B. Pujari, *Ann. Afr. Med.* **2019**, *18*, 121-126.

[3] F. R. Greten, S. I. Grivennikov, *Immunity* **2019**, *51*, 27-41.

[4] M. Metzemaekers, B. Malengier-Devlies, M. Gouwy, M.; L. De Somer, F. de Queiroz Cunha, G. Opdenakker, P. Proost, *Med. Res. Rev.* **2023**, 1-70.

[5] I. Piotrowskia, K. Kulcentya, W. Suchorska, *Rep. Pract. Oncol. Radiother*. **2020**, *25*, 422-427.

[6] Y. Zhang, W. Kong, J. Jiang, *Sci China Life Sci.* **2017**, *60*, 601-616.

[7] A. A. Abu-Hashem, S. A. Al-Hussain, M. E. A. Zaki, *Molecules* **2021**, *26*, 2031.

[8] A. A. Abu-Hashem, *J. Heterocycl. Chem.* **2021**, *58*, 805-821.

[9] A. Bruno, C. Brullo, F. Bondavalli, A. Ranise, S. Schenone, M. S. Falzarano, K. Varani, S. Spisani, *Bioorg. Med. Chem. Lett.* **2007**, *17*, 3696-3701.

[10] E. Meta, C. Brullo, A. Sidibè, B. A. Imhof, O. Bruno, *Eur. J. Med. Chem.* **2017**, *133*, 24-35.

[11] M. G. Signorello, F. Rapetti, E. Meta, A. Sidibè, O. Bruno, C Brullo, *Molecules* **2021**, *26*, 5735-5755.

[12] B. Marengo, E. Meta, C. Brullo, C. De Ciucis, R. Colla, A. Speciale, O. Garbarino, O. Bruno, C. Domenicotti, *Oncotarget* **2023**, *14,* 129-130.

[13] T. Qin, F. Chen, X. Zhuo, X. Guo, T. Yun, Y. Liu, C. Zhang, L. Lai, *J. Med. Chem.* **2016**, *59*, 7089-7096.

[14] D. A. Rodrigues, G. A. Ferreira-Silva, A. C. S. Ferreira, R. A. J. Fernandes, K. Kwee, C. M. R. Sant’Anna, M. Ionta, C. A: M. Fraga, *J. Med. Chem.* **2016**, *59*, 655-670.

[15] W. J. Zuercher, S. Gaillard, L. A. Orband-Miller, E. Y. H. Chao, B. G. Shearer, D.G. Jones, A. B. Miller, J. L. Collins, D. P. McDonnell, T. M. Willson, *J. Med. Chem.* **2005**, *48*, 3107-3109.

[16] C. Brullo, F. Rapetti, S. Alfei, I. Maric, F. Rizzelli, M. Mapelli, C. Rosano, M. Viale, O. Bruno, *ChemMedChem* **2020**, *15*, 961-969.

[17] C. Brullo, M. Massa, F. Rapetti, S. Alfei, M. B. Bertolotto, F. Montecucco, M. G. Signorello, O. Bruno, *Molecules* **2020**, *25*, 899-917.

[18] G. Benoit, *Bull. Soc. Chim. Fr.* **1939**, *6*, 708.

[19] S. Schenone, O. Bruno, P. Fossa, A. Ranise, G. Menozzi, L. Mosti, F. Bondavalli, C. Martini, L. Trincavelli, *Bioorg. Med. Chem. Lett.* **2001**, *11*, 2529-2531.

[20] S. J. Zuo, S. Li, R. H. Yu, G. X. Zheng, Y. X. Cao, S. Q. Zhang, *Bioorg. Med. Chem. Lett.* **2014**, *24*, 5597-5601.

[21] T. Lampe, C. Alonso-Alija, B. Stelte-ludwig, P. Sandner, M. Bauser, H. Beck, K. Lustig, U. Rosentreter, E. Stahl, H. Takagi (Bayer Healthcare AG) WO 2006040136, **2006**.

[22] M. J. Ashton, D. C. Cook, G. H. Fenton, S. J. Hills, I. M. Mcfarlane, M. N. Palfreyman, A. J. Ratcliffe, N Vicker (Aventis Pharma) EP497564, **1992**.

[23] C. Brullo, M. Massa, C. Villa, R. Ricciarelli, D. Rivera, M. A. Pronzato, E. Fedele, E. Barocelli, S. Bertoni, L. Flammini, O. Bruno, *Bioorg. Med. Chem.* **2015**, *23*, 3426-3435.

[24] E. Hernández-Vázqueza, R. Castañeda-Arriaga, J. Ramírez-Espinosad, O. N. Medina-Campos, F. Hernández-Luis, J. P. Chaverri, S. Estrada-Soto, *Eur. J. Med. Chem.* **2015**, *100*, 106-116.

[25] A. T. Franco, A. Corken, J. Ware, *Blood* **2015**, *126*, 582-588.

[26] M. Mittal, M. R. Siddiqui, K. Tran, S. P. Reddy, A. B. Malik, *Antioxid. Redox Signal.* **2014**, *20*, 1126-1167.

[27] E. Sierko, M. Z. Wojtukiewicz, *Semin. Thromb. Hemost.* **2004**, *30*, 95-108.

[28] A. Daina, O. Michielin, V. Zoete, *Sci. Rep.* **2017**, *7*, 42717-42729.

[29] J. S. Delaney, *J. Chem. Inf. Model.* **2004**, *44*, 1000-1005.

[30] R. Brenk, A. Schipani, D. James, A. Krasowski, I. H. Gilbert, J. Frearson, P. G. Wyatt, *ChemMedChem* **2008**, *3*, 435-444.

[31] H. Chen, S. Deng, N. Albadari, M. K. Yun, S. Zhang, Y. Li, D. Ma, D. N. Parke, L. Yang, T. N. Seagroves, S. W. White, D. D. Miller, W. Li, *J. Med. Chem.* **2021**, *64*, 12049-12074.

[32] G. M. Morris, R. Huey, W. Lindstrom, M. F. Sanner, R. K. Belew, D. S. Goodsell, A. J. Olson, *J. Comput. Chem.* **2009**, *17*, 2785-2791.

[33] M. Mohammadgholi, S. J. Hosseinimehr, *Curr Med Chem*. **2023**, 10.2174/0929867330666230407104208

[34] Q. Cui, J. Q. Wang, Y. G. Assaraf, L. Ren, P. Gupta, L. Wei, C. R. Ashby, D. H. Yang, Z. S. Chen, *Drug Resist. Updates* **2018**, *41*, 1–25.

[35] B. Perillo, M. Di Donato, A. Pezone, E. Di Zazzo, P. Giovannelli, G. Galasso, G. Castoria, A. Migliaccio, *Exp. Mol. Med.* **2020**, *52*, 192–203.

[36] L. Chen, H. Deng, H. Cui, J. Fang, Z. Zuo, J. Deng, Y. Li, X. Wang, L. Zhao, *Oncotarget* **2017**, *9*, 7204–7218.

[37] H. Zhao, L. Wu, G. Yan, Y. Yu Chen, M. Zhou, Y. Wu, Y. Li, *Signal Trans. Targ. Ther.* **2021**, *6*, 263.

[38] V. Ramundo, G. Giribaldi, E. Aldieri, *Cancers* **2021**, *13,* 3093.

[39] D. L. Flynn, M. D. Kaufman, (Deciphera Pharmaceuticals, LLC) WO 2011139891, **2011**.

[40] G. V. R. Born, *Nature* **1962**, *194*, 927-929.

[41] M. D. Winn, C. C. Ballard, K. D. Cowtan, E. J. Dodson, P. Emsley, P. R. Evans, R. M. Keegan, E. B. Krissinel, A. G. W. Leslie, A. McCoy, J. M. Stuart, G. N. Murshudov, N. S: Pannu, E. A. Potterton, H. R. Powell, R. J. Read, A. Vagin, K. S. Wilson, *Acta Crystallogr. Sect. D. Biol. Crystallogr.* **2011**, *67*, 235-242.

[42] S. Jo, T. Kim, V. G. Iyer, W. Im, *J. Comput. Chem.* **2008**, *29*, 1859-1865.

[43] W. Humphrey, A. Dalke, K. Schulten, *J. Molec. Graphics* **1996**, *14*, 33-38.

[44] J. C. Phillips, D. J. Hardy, J. D. C. Maia, J. E. Stone, J. V. Ribeiro, R. C. Bernardi, R. Buch, G. Fiorin, J. Henin, W. Jiang, R. McGreevy, M. C. R. Melo, B. K. Radak, D. Skeel, A. Singharoy, Y. Wang, B. Roux, A. Aksimentiev, Z. Luthey-Schulten, L. V. Kale, K. Schulten, C. Chipot, E. Tajkhorshid, *J. Chem. Phys.* **2020**, *153*, 044130.

Table of Contents

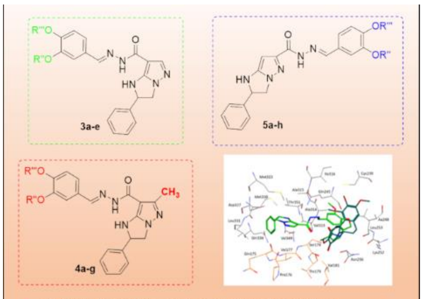
R''O
R''O
3a-e
OR'''
OR''
5a-h
R'''O
R''O
CH3
4a-g

- Anti-proliferative and antioxidant activities
- Computational simulations on tubulin system
- In silico DMPK properties